MAE 5870 - Aula 4

Regressão em Séries Temporais – domínio de tempo

2.2 Classical Regression in the Time Series Context

We begin our discussion of linear regression in the time series context by assuming some output or dependent time series, say, x_t, for $t = 1, \ldots, n$, is being influenced by a collection of possible inputs or independent series, say, $z_{t1}, z_{t2}, \ldots, z_{tq}$, where we first regard the inputs as fixed and known. This assumption, necessary for applying conventional linear regression, will be relaxed later on. We express this relation through the linear regression model

$$x_t = \beta_1 z_{t1} + \beta_2 z_{t2} + \cdots + \beta_q z_{tq} + w_t, \tag{2.1}$$

where $\beta_1, \beta_2, \ldots, \beta_q$ are unknown fixed regression coefficients, and $\{w_t\}$ is a random error or noise process consisting of independent and identically distributed (iid) normal variables with mean zero and variance σ_w^2; we will relax the iid assumption later.

Example 2.1 Estimating a Linear Trend

Consider the global temperature data, say x_t, shown in Figures 1.2 and 2.1. As discussed in Example 1.2, there is an apparent upward trend in the series that has been used to argue the global warming hypothesis. We might use simple linear regression to estimate that trend by fitting the model

$$x_t = \beta_1 + \beta_2 t + w_t, \quad t = 1880, 1857, \ldots, 2009.$$

$$\widehat{x}_t = -11.2 + .006t$$

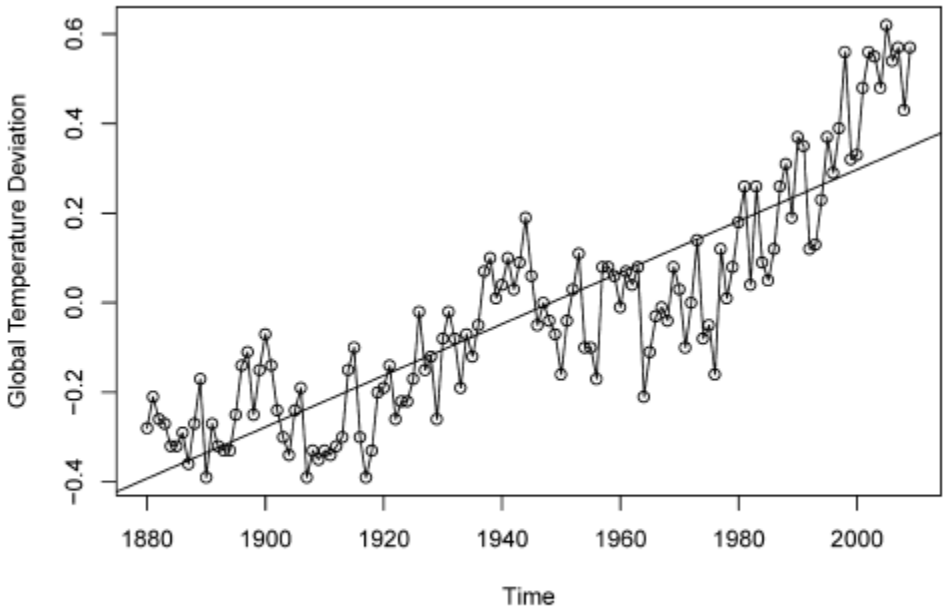

Fig. 2.1. Global temperature deviations shown in Figure 1.2 with fitted linear trend line.

The linear model described by (2.1) above can be conveniently written in a more general notation by defining the column vectors $\boldsymbol{z}_t = (z_{t1}, z_{t2}, \ldots, z_{tq})'$ and $\boldsymbol{\beta} = (\beta_1, \beta_2, \ldots, \beta_q)'$, where $'$ denotes transpose, so (2.1) can be written in the alternate form

$$x_t = \boldsymbol{\beta}' \boldsymbol{z}_t + w_t. \tag{2.2}$$

where $w_t \sim$ iid $\mathrm{N}(0, \sigma_w^2)$. It is natural to consider estimating the unknown coefficient vector $\boldsymbol{\beta}$ by minimizing the error sum of squares

$$Q = \sum_{t=1}^{n} w_t^2 = \sum_{t=1}^{n} (x_t - \boldsymbol{\beta}' \boldsymbol{z}_t)^2, \tag{2.3}$$

with respect to $\beta_1, \beta_2, \ldots, \beta_q$. Minimizing Q yields the ordinary least squares estimator of $\boldsymbol{\beta}$. This minimization can be accomplished by differentiating (2.3) with respect to the vector $\boldsymbol{\beta}$ or by using the properties of projections. In the notation above, this procedure gives the normal equations

$$\left(\sum_{t=1}^{n} \boldsymbol{z}_t \boldsymbol{z}_t' \right) \widehat{\boldsymbol{\beta}} = \sum_{t=1}^{n} \boldsymbol{z}_t x_t. \tag{2.4}$$

The notation can be simplified by defining $Z = [\boldsymbol{z}_1 \,|\, \boldsymbol{z}_2 \,|\, \cdots \,|\, \boldsymbol{z}_n]'$ as the $n \times q$ matrix composed of the n samples of the input variables, the observed $n \times 1$ vector $\boldsymbol{x} = (x_1, x_2, \ldots, x_n)'$ and the $n \times 1$ vector of errors

$\boldsymbol{w} = (w_1, w_2, \ldots, w_n)'$. In this case, model (2.2) may be written as

$$\boldsymbol{x} = Z\boldsymbol{\beta} + \boldsymbol{w}. \tag{2.5}$$

The normal equations, (2.4), can now be written as

$$(Z'Z)\,\widehat{\boldsymbol{\beta}} = Z'\boldsymbol{x} \tag{2.6}$$

and the solution

$$\widehat{\boldsymbol{\beta}} = (Z'Z)^{-1}Z'\boldsymbol{x} \tag{2.7}$$

when the matrix $Z'Z$ is nonsingular. The minimized error sum of squares (2.3), denoted SSE, can be written as

$$\begin{aligned} SSE &= \sum_{t=1}^{n}(x_t - \widehat{\boldsymbol{\beta}}'\boldsymbol{z}_t)^2 \\ &= (\boldsymbol{x} - Z\widehat{\boldsymbol{\beta}})'(\boldsymbol{x} - Z\widehat{\boldsymbol{\beta}}) \\ &= \boldsymbol{x}'\boldsymbol{x} - \widehat{\boldsymbol{\beta}}'Z'\boldsymbol{x} \\ &= \boldsymbol{x}'\boldsymbol{x} - \boldsymbol{x}'Z(Z'Z)^{-1}Z'\boldsymbol{x}, \end{aligned} \tag{2.8}$$

to give some useful versions for later reference. The ordinary least squares estimators are unbiased, i.e., $E(\widehat{\boldsymbol{\beta}}) = \boldsymbol{\beta}$, and have the smallest variance within the class of linear unbiased estimators.

If the errors w_t are normally distributed, $\widehat{\boldsymbol{\beta}}$ is also the maximum likelihood estimator for $\boldsymbol{\beta}$ and is normally distributed with

$$\operatorname{cov}(\widehat{\boldsymbol{\beta}}) = \sigma_w^2 \left(\sum_{t=1}^{n} \boldsymbol{z}_t \boldsymbol{z}_t' \right)^{-1} = \sigma_w^2 (Z'Z)^{-1} = \sigma_w^2 C, \tag{2.9}$$

where

$$C = (Z'Z)^{-1} \tag{2.10}$$

is a convenient notation for later equations. An unbiased estimator for the variance σ_w^2 is

$$s_w^2 = MSE = \frac{SSE}{n-q}, \tag{2.11}$$

where MSE denotes the *mean squared error*, which is contrasted with the maximum likelihood estimator $\widehat{\sigma}_w^2 = SSE/n$. Under the normal assumption, s_w^2 is distributed proportionally to a chi-squared random variable with $n-q$ degrees of freedom, denoted by χ_{n-q}^2, and independently of $\widehat{\beta}$. It follows that

$$t_{n-q} = \frac{(\widehat{\beta}_i - \beta_i)}{s_w \sqrt{c_{ii}}} \tag{2.12}$$

has the t-distribution with $n-q$ degrees of freedom; c_{ii} denotes the i-th diagonal element of C, as defined in (2.10).

Various competing models are of interest to isolate or select the best subset of independent variables. Suppose a proposed model specifies that only a subset $r < q$ independent variables, say, $\boldsymbol{z}_{t:r} = (z_{t1}, z_{t2}, \ldots, z_{tr})'$ is influencing the dependent variable x_t. The reduced model is

$$\boldsymbol{x} = Z_r \boldsymbol{\beta}_r + \boldsymbol{w} \tag{2.13}$$

where $\boldsymbol{\beta}_r = (\beta_1, \beta_2, \ldots, \beta_r)'$ is a subset of coefficients of the original q variables and $Z_r = [\boldsymbol{z}_{1:r} \mid \cdots \mid \boldsymbol{z}_{n:r}]'$ is the $n \times r$ matrix of inputs. The null hypothesis in this case is H_0: $\beta_{r+1} = \cdots = \beta_q = 0$. We can test the reduced model (2.13) against the full model (2.2) by comparing the error sums of squares under the two models using the F-statistic

$$F_{q-r,n-q} = \frac{(SSE_r - SSE)/(q-r)}{SSE/(n-q)}, \tag{2.14}$$

which has the central F-distribution with $q-r$ and $n-q$ degrees of freedom when (2.13) is the correct model. Note that SSE_r is the error sum of squares under the reduced model (2.13) and it can be computed by replacing Z with Z_r in (2.8). The statistic, which follows from applying the likelihood ratio criterion, has the improvement per number of parameters added in the numerator compared with the error sum of squares under the full model in the denominator. The information involved in the test procedure is often summarized in an Analysis of Variance (ANOVA) table as given in Table 2.1 for this particular case. The difference in the numerator is often called the regression sum of squares

Table 2.1. Analysis of Variance for Regression

Source	df	Sum of Squares	Mean Square
$z_{t,r+1}, \ldots, z_{t,q}$	$q-r$	$SSR = SSE_r - SSE$	$MSR = SSR/(q-r)$
Error	$n-q$	SSE	$MSE = SSE/(n-q)$
Total	$n-r$	SSE_r	

In terms of Table 2.1, it is conventional to write the F-statistic (2.14) as the ratio of the two mean squares, obtaining

$$F_{q-r,n-q} = \frac{MSR}{MSE}, \tag{2.15}$$

where MSR, the *mean squared regression*, is the numerator of (2.14). A special case of interest is $r = 1$ and $z_{t1} \equiv 1$, when the model in (2.13) becomes

$$x_t = \beta_1 + w_t,$$

and we may measure the proportion of variation accounted for by the other variables using

$$R^2 = \frac{SSE_1 - SSE}{SSE_1}, \tag{2.16}$$

where the residual sum of squares under the reduced model

$$SSE_1 = \sum_{t=1}^{n} (x_t - \bar{x})^2, \tag{2.17}$$

in this case is just the sum of squared deviations from the mean $\bar{x}$. The measure R^2 is also the *squared multiple correlation* between x_t and the variables $z_{t2}, z_{t3}, \ldots, z_{tq}$.

Critério de seleção

Suppose we consider a normal regression model with k coefficients and denote the maximum likelihood estimator for the variance as

$$\widehat{\sigma}_k^2 = \frac{SSE_k}{n}, \tag{2.18}$$

where SSE_k denotes the residual sum of squares under the model with k regression coefficients. Then, Akaike (1969, 1973, 1974) suggested measuring the goodness of fit for this particular model by balancing the error of the fit against the number of parameters in the model; we define the following.[1]

Definition 2.1 Akaike's Information Criterion (AIC)

$$\text{AIC} = \log\ \widehat{\sigma}_k^2 + \frac{n+2k}{n}, \tag{2.19}$$

where $\widehat{\sigma}_k^2$ is given by (2.18) and k is the number of parameters in the model.

Definition 2.2 AIC, Bias Corrected (AICc)

$$\text{AICc} = \log\ \widehat{\sigma}_k^2 + \frac{n+k}{n-k-2}, \tag{2.20}$$

where $\widehat{\sigma}_k^2$ is given by (2.18), k is the number of parameters in the model, and n is the sample size.

We may also derive a correction term based on Bayesian arguments, as in Schwarz (1978), which leads to the following.

Definition 2.3 Bayesian Information Criterion (BIC)

$$\text{BIC} = \log\ \widehat{\sigma}_k^2 + \frac{k \log n}{n}, \tag{2.21}$$

using the same notation as in Definition 2.2.

BIC is also called the Schwarz Information Criterion (SIC); see also Rissanen (1978) for an approach yielding the same statistic based on a minimum description length argument. Various simulation studies have tended to verify that BIC does well at getting the correct order in large samples, whereas AICc tends to be superior in smaller samples where the relative number of parameters is large; see McQuarrie and Tsai (1998) for detailed comparisons. In fitting regression models, two measures that have been used in the past are adjusted R-squared, which is essentially s_w^2, and Mallows C_p, Mallows (1973), which we do not consider in this context.

Example 2.2 Pollution, Temperature and Mortality

The data shown in Figure 2.2 are extracted series from a study by Shumway et al. (1988) of the possible effects of temperature and pollution on weekly mortality in Los Angeles County. Note the strong seasonal components in all of the series, corresponding to winter-summer variations and the downward trend in the cardiovascular mortality over the 10-year period.

A scatterplot matrix, shown in Figure 2.3, indicates a possible linear relation between mortality and the pollutant particulates and a possible relation to temperature. Note the curvilinear shape of the temperature mortality curve, indicating that higher temperatures as well as lower temperatures are associated with increases in cardiovascular mortality.

Based on the scatterplot matrix, we entertain, tentatively, four models where M_t denotes cardiovascular mortality, T_t denotes temperature and P_t denotes the particulate levels. They are

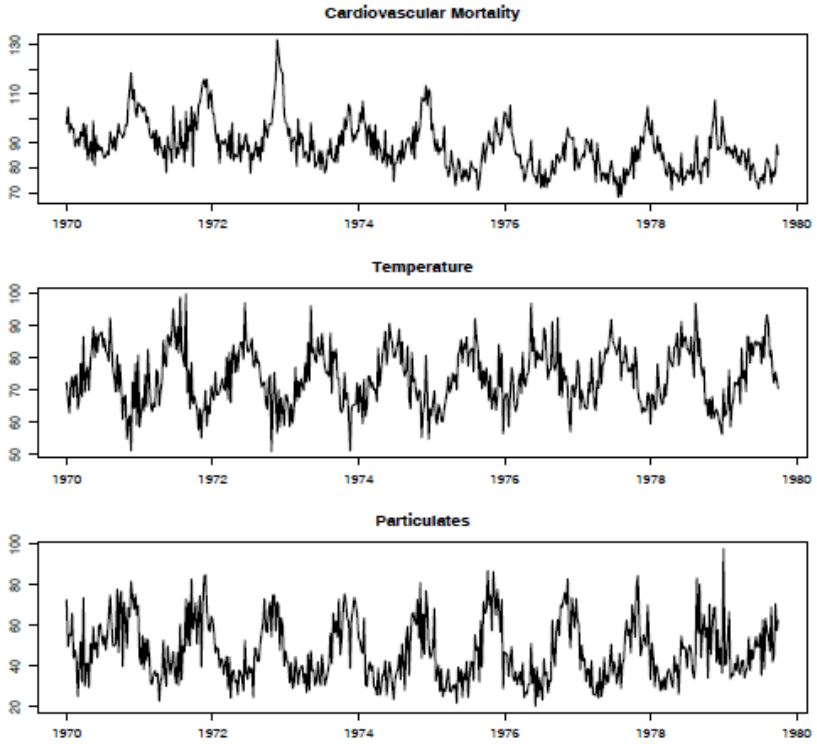

Fig. 2.2. Average weekly cardiovascular mortality (top), temperature (middle) and particulate pollution (bottom) in Los Angeles County. There are 508 six-day smoothed averages obtained by filtering daily values over the 10 year period 1970-1979.

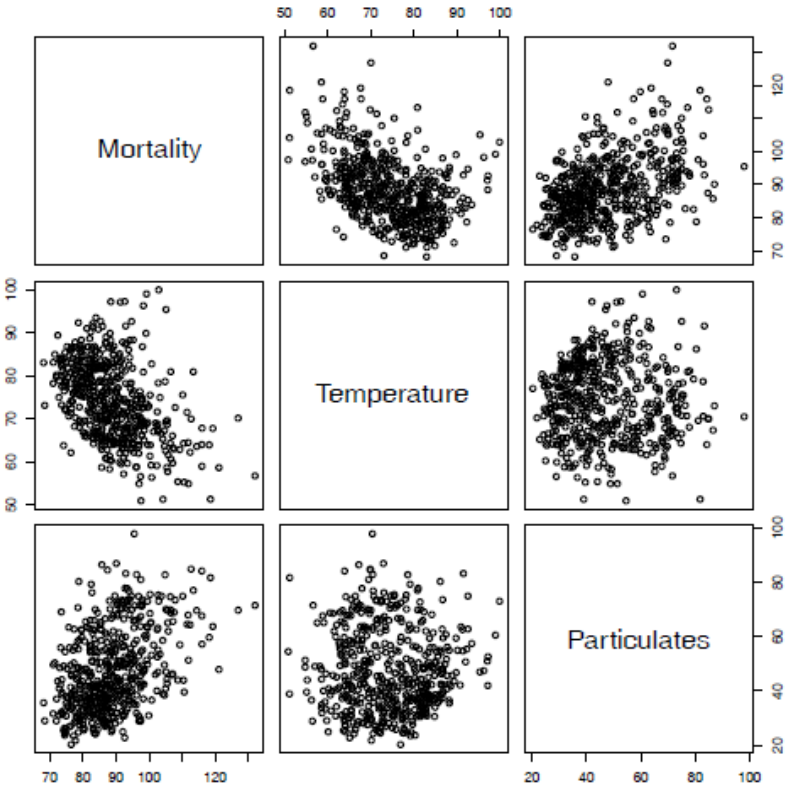

Fig. 2.3. Scatterplot matrix showing plausible relations between mortality, temperature, and pollution.

$$M_t = \beta_1 + \beta_2 t + w_t \tag{2.22}$$
$$M_t = \beta_1 + \beta_2 t + \beta_3(T_t - T.) + w_t \tag{2.23}$$
$$M_t = \beta_1 + \beta_2 t + \beta_3(T_t - T.) + \beta_4(T_t - T.)^2 + w_t \tag{2.24}$$
$$M_t = \beta_1 + \beta_2 t + \beta_3(T_t - T.) + \beta_4(T_t - T.)^2 + \beta_5 P_t + w_t \tag{2.25}$$

where we adjust temperature for its mean, $T. = 74.6$, to avoid scaling problems. It is clear that (2.22) is a trend only model, (2.23) is linear temperature, (2.24) is curvilinear temperature and (2.25) is curvilinear temperature and pollution. We summarize some of the statistics given for this particular case in Table 2.2. The values of R^2 were computed by noting that $SSE_1 = 50,687$ using (2.17).

Table 2.2. Summary Statistics for Mortality Models

Model	k	SSE	df	MSE	R^2	AIC	BIC
(2.22)	2	40,020	506	79.0	.21	5.38	5.40
(2.23)	3	31,413	505	62.2	.38	5.14	5.17
(2.24)	4	27,985	504	55.5	.45	5.03	5.07
(2.25)	5	20,508	503	40.8	.60	4.72	4.77

We note that each model does substantially better than the one before it and that the model including temperature, temperature squared, and particulates does the best, accounting for some 60% of the variability and with the best value for AIC and BIC (because of the large sample size, AIC and AICc are nearly the same). Note that one can compare any two models using the residual sums of squares and (2.14). Hence, a model with only trend could be compared to the full model using $q = 5, r = 2, n = 508$, so

$$F_{3,503} = \frac{(40,020 - 20,508)/3}{20,508/503} = 160,$$

which exceeds $F_{3,503}(.001) = 5.51$. We obtain the best prediction model,

$$\begin{aligned}\widehat{M}_t = 81.59 &- .027_{(.002)}t - .473_{(.032)}(T_t - 74.6) \\ &+ .023_{(.003)}(T_t - 74.6)^2 + .255_{(.019)}P_t,\end{aligned}$$

for mortality, where the standard errors, computed from (2.9)-(2.11), are given in parentheses. As expected, a negative trend is present in time as well as a negative coefficient for adjusted temperature. The quadratic effect of temperature can clearly be seen in the scatterplots of Figure 2.3. Pollution weights positively and can be interpreted as the incremental contribution to daily deaths per unit of particulate pollution. It would still be essential to check the residuals $\widehat{w}_t = M_t - \widehat{M}_t$ for autocorrelation (of which there is a substantial amount), but we defer this question to to §5.6 when we discuss regression with correlated errors.

Example 2.3 Regression With Lagged Variables

In Example 1.25, we discovered that the Southern Oscillation Index (SOI) measured at time $t - 6$ months is associated with the Recruitment series at time t, indicating that the SOI leads the Recruitment series by six months. Although there is evidence that the relationship is not linear (this is discussed further in Example 2.7), we may consider the following regression,

$$R_t = \beta_1 + \beta_2 S_{t-6} + w_t, \tag{2.26}$$

where R_t denotes Recruitment for month t and S_{t-6} denotes SOI six months prior. Assuming the w_t sequence is white, the fitted model is

$$\widehat{R}_t = 65.79 - 44.28_{(2.78)}S_{t-6} \tag{2.27}$$

with $\widehat{\sigma}_w = 22.5$ on 445 degrees of freedom. This result indicates the strong predictive ability of SOI for Recruitment six months in advance. Of course, it is still essential to check the the model assumptions, but again we defer this until later.

Exploratory Data Analysis

In general, it is necessary for time series data to be stationary, so averaging lagged products over time will be a sensible thing to do.

With time series data, it is the dependence between the values of the series that is important to measure; we must, at least, be able to estimate autocorrelations with precision.

It would be difficult to measure that dependence if the dependence structure is not regular or is changing at every time point. Hence, to achieve any meaningful statistical analysis of time series data, it will be crucial that, if nothing else, the mean and the autocovariance functions satisfy the conditions of stationarity

Often, this is not the case, and we will mention some methods for playing down the effects of nonstationarity so the stationary properties of the series may be studied.

Examples:

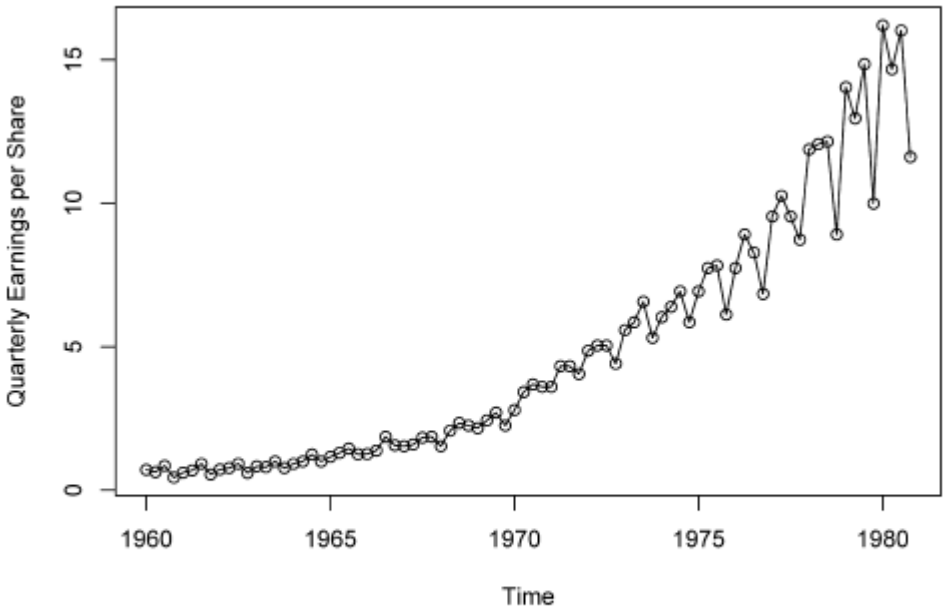

Fig. 1.1. Johnson & Johnson quarterly earnings per share, 84 quarters, 1960-I to 1980-IV.

Example 2.4 Detrending Global Temperature

Here we suppose the model is of the form of (2.28),

$$x_t = \mu_t + y_t,$$

where, as we suggested in the analysis of the global temperature data presented in Example 2.1, a straight line might be a reasonable model for the trend, i.e.,

$$\mu_t = \beta_1 + \beta_2\, t.$$

In that example, we estimated the trend using ordinary least squares[3] and found

$$\widehat{\mu}_t = -11.2 + .006\, t.$$

where w_t is white noise and is independent of y_t. If the appropriate model is (2.28), then differencing the data, x_t, yields a stationary process; that is,

$$\begin{aligned} x_t - x_{t-1} &= (\mu_t + y_t) - (\mu_{t-1} + y_{t-1}) \\ &= \delta + w_t + y_t - y_{t-1}. \end{aligned} \tag{2.31}$$

It is easy to show $z_t = y_t - y_{t-1}$ is stationary using footnote 3 of Chapter 1 on page 20. That is, because y_t is stationary,

$$\begin{aligned} \gamma_z(h) &= \text{cov}(z_{t+h}, z_t) = \text{cov}(y_{t+h} - y_{t+h-1}, y_t - y_{t-1}) \\ &= 2\gamma_y(h) - \gamma_y(h+1) - \gamma_y(h-1) \end{aligned}$$

is independent of time; we leave it as an exercise (Problem 2.7) to show that $x_t - x_{t-1}$ in (2.31) is stationary.

In Example 1.11 and the corresponding Figure 1.10 we saw that a random walk might also be a good model for trend. That is, rather than modeling trend as fixed (as in Example 2.4), we might model trend as a stochastic component using the random walk with drift model,

$$\mu_t = \delta + \mu_{t-1} + w_t, \tag{2.30}$$

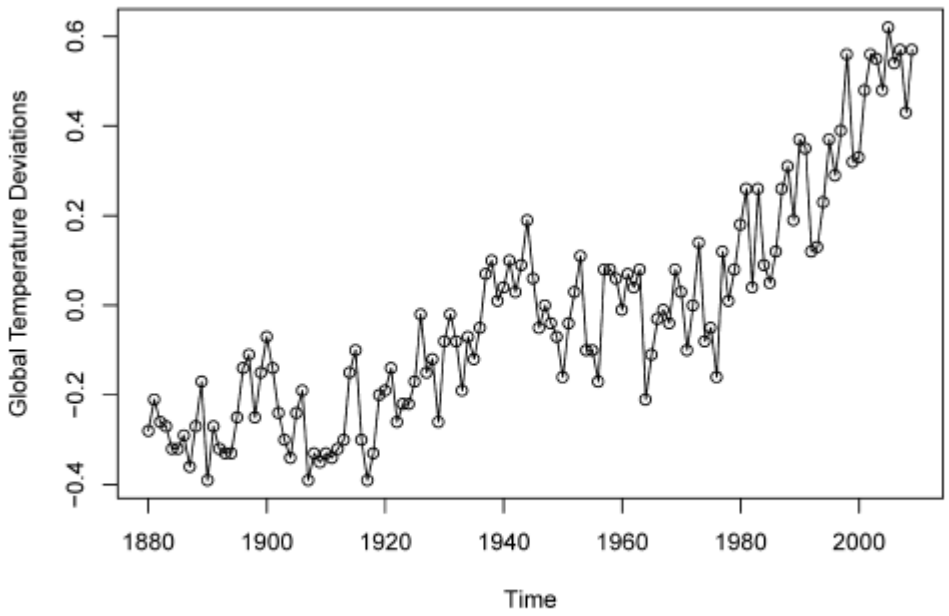

Fig. 1.2. Yearly average global temperature deviations (1880–2009) in degrees centigrade.

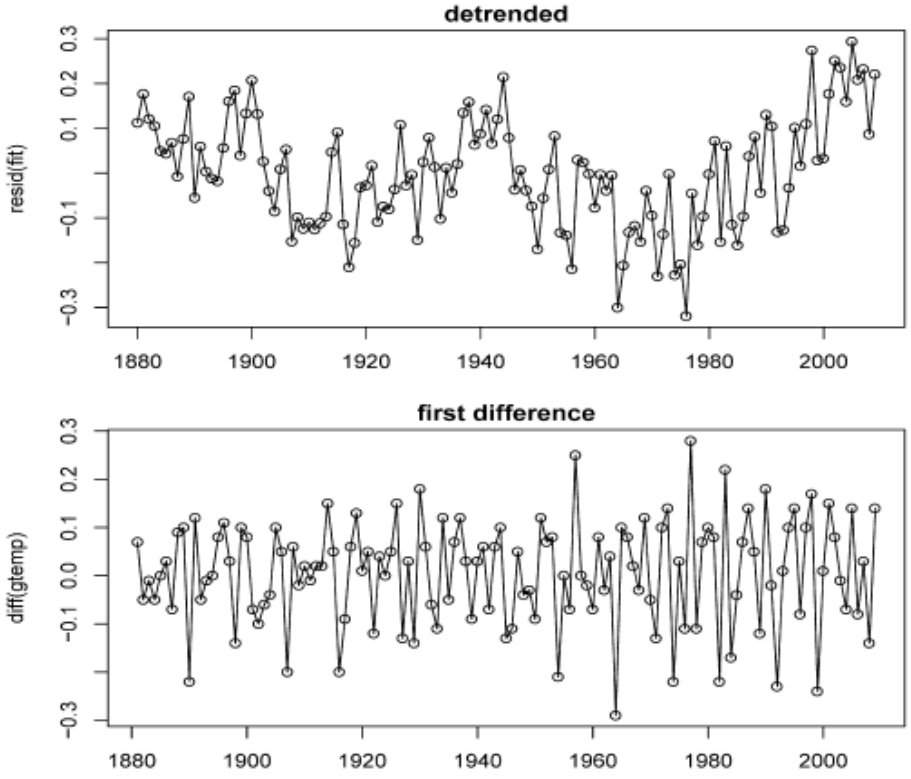

Fig. 2.4. Detrended (top) and differenced (bottom) global temperature series. The original data are shown in Figures 1.2 and 2.1.

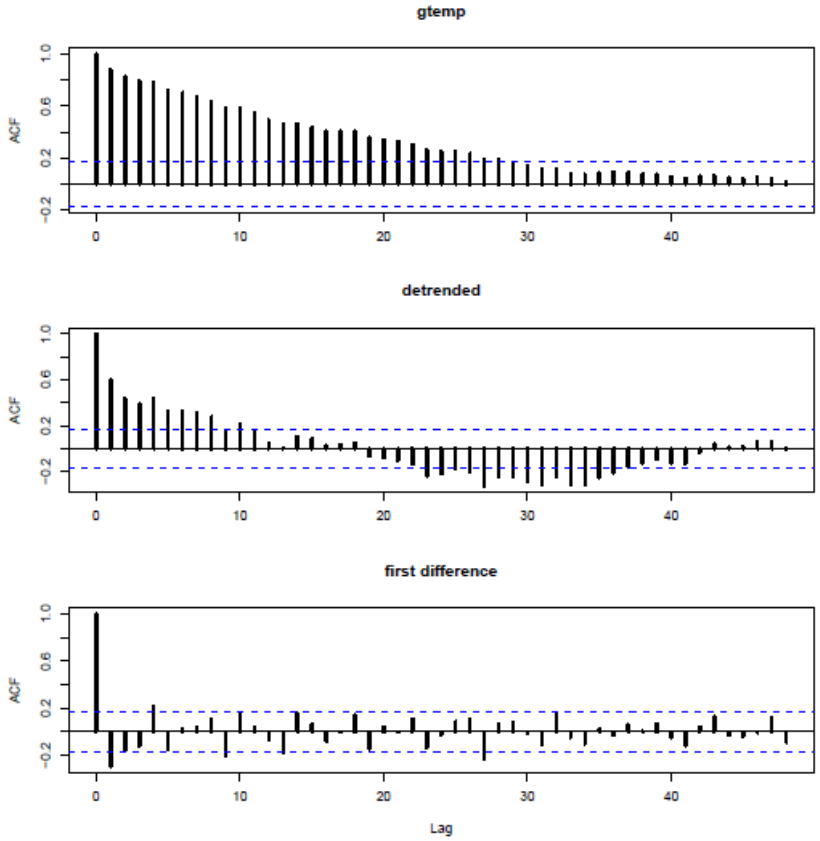

Fig. 2.5. Sample ACFs of the global temperature (top), and of the detrended (middle) and the differenced (bottom) series.

Definition 2.4 *We define the* **backshift operator** *by*

$$Bx_t = x_{t-1}$$

and extend it to powers $B^2x_t = B(Bx_t) = Bx_{t-1} = x_{t-2}$, *and so on. Thus,*

$$B^k x_t = x_{t-k}. \tag{2.33}$$

It is clear that we may then rewrite (2.32) as

$$\nabla x_t = (1 - B)x_t, \tag{2.34}$$

and we may extend the notion further. For example, the second difference becomes

$$\begin{aligned}\nabla^2 x_t &= (1 - B)^2 x_t = (1 - 2B + B^2)x_t \\ &= x_t - 2x_{t-1} + x_{t-2}\end{aligned}$$

by the linearity of the operator. To check, just take the difference of the first difference $\nabla(\nabla x_t) = \nabla(x_t - x_{t-1}) = (x_t - x_{t-1}) - (x_{t-1} - x_{t-2})$.

Definition 2.5 Differences of order d *are defined as*

$$\nabla^d = (1 - B)^d, \tag{2.35}$$

where we may expand the operator $(1-B)^d$ *algebraically to evaluate for higher integer values of* d. *When* $d = 1$, *we drop it from the notation.*

Often, obvious aberrations are present that can contribute nonstationary as well as nonlinear behavior in observed time series. In such cases, transformations may be useful to equalize the variability over the length of a single series. A particularly useful transformation is

$$y_t = \log x_t, \tag{2.36}$$

which tends to suppress larger fluctuations that occur over portions of the series where the underlying values are larger. Other possibilities are power transformations in the Box–Cox family of the form

$$y_t = \begin{cases} (x_t^\lambda - 1)/\lambda & \lambda \neq 0, \\ \log x_t & \lambda = 0. \end{cases} \tag{2.37}$$

Methods for choosing the power λ are available (see Johnson and Wichern, 1992, §4.7) but we do not pursue them here. Often, transformations are also used to improve the approximation to normality or to improve linearity in predicting the value of one series from another.

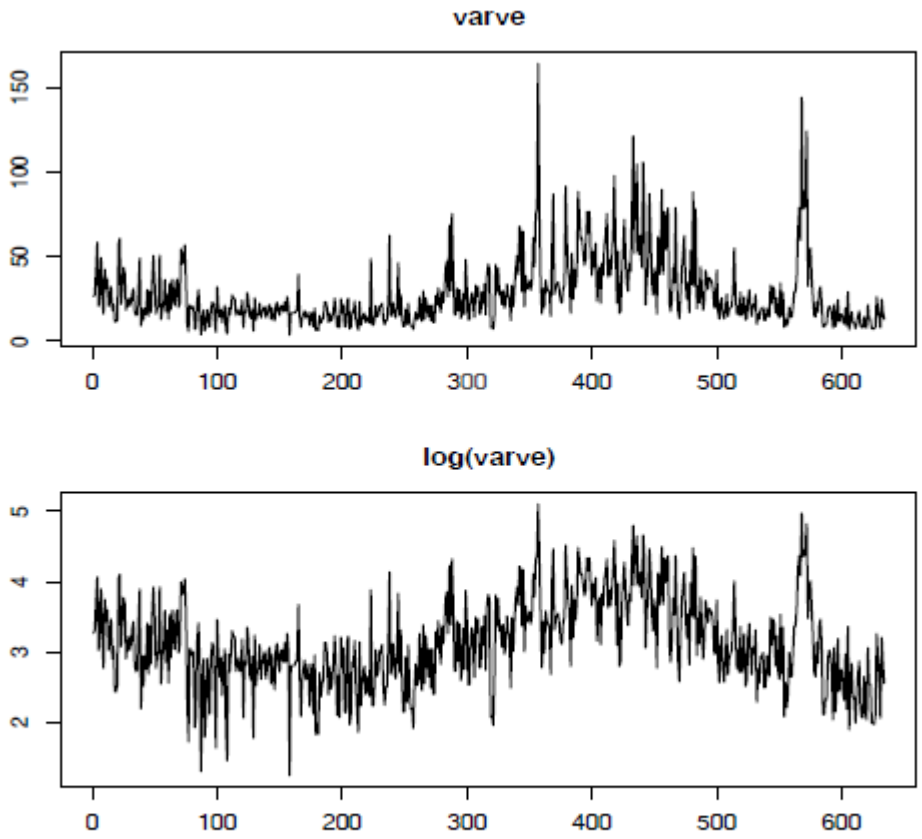

Fig. 2.6. Glacial varve thicknesses (top) from Massachusetts for $n = 634$ years compared with log transformed thicknesses (bottom).

Example 2.6 Paleoclimatic Glacial Varves

Melting glaciers deposit yearly layers of sand and silt during the spring melting seasons, which can be reconstructed yearly over a period ranging from the time deglaciation began in New England (about 12,600 years ago) to the time it ended (about 6,000 years ago). Such sedimentary deposits, called varves, can be used as proxies for paleoclimatic parameters, such as temperature, because, in a warm year, more sand and silt are deposited from the receding glacier. Figure 2.6 shows the thicknesses of the yearly varves collected from one location in Massachusetts for 634 years, beginning 11,834 years ago. For further information, see Shumway and Verosub (1992). Because the variation in thicknesses increases in proportion to the amount deposited, a logarithmic transformation could remove the nonstationarity observable in the variance as a function of time. Figure 2.6 shows the original and transformed varves, and it is clear that this improvement has occurred.

Example 2.7 Scatterplot Matrices, SOI and Recruitment

To check for nonlinear relations of this form, it is convenient to display a lagged scatterplot matrix, as in Figure 2.7, that displays values of the SOI, S_t, on the vertical axis plotted against S_{t-h} on the horizontal axis. The sample autocorrelations are displayed in the upper right-hand corner and superimposed on the scatterplots are locally weighted scatterplot smoothing (lowess) lines that can be used to help discover any nonlinearities. We discuss smoothing in the next section, but for now, think of lowess as a robust method for fitting nonlinear regression.

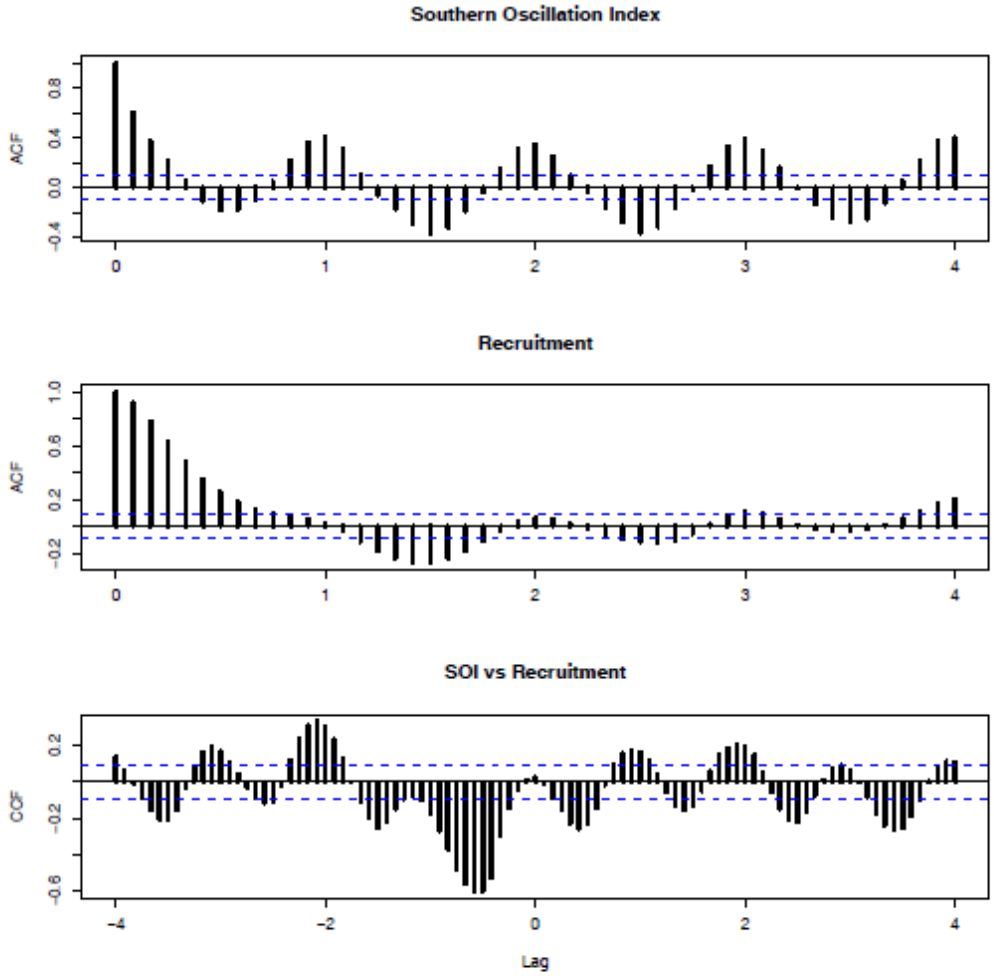

Fig. 1.14. Sample ACFs of the SOI series (top) and of the Recruitment series (middle), and the sample CCF of the two series (bottom); negative lags indicate SOI leads Recruitment. The lag axes are in terms of seasons (12 months).

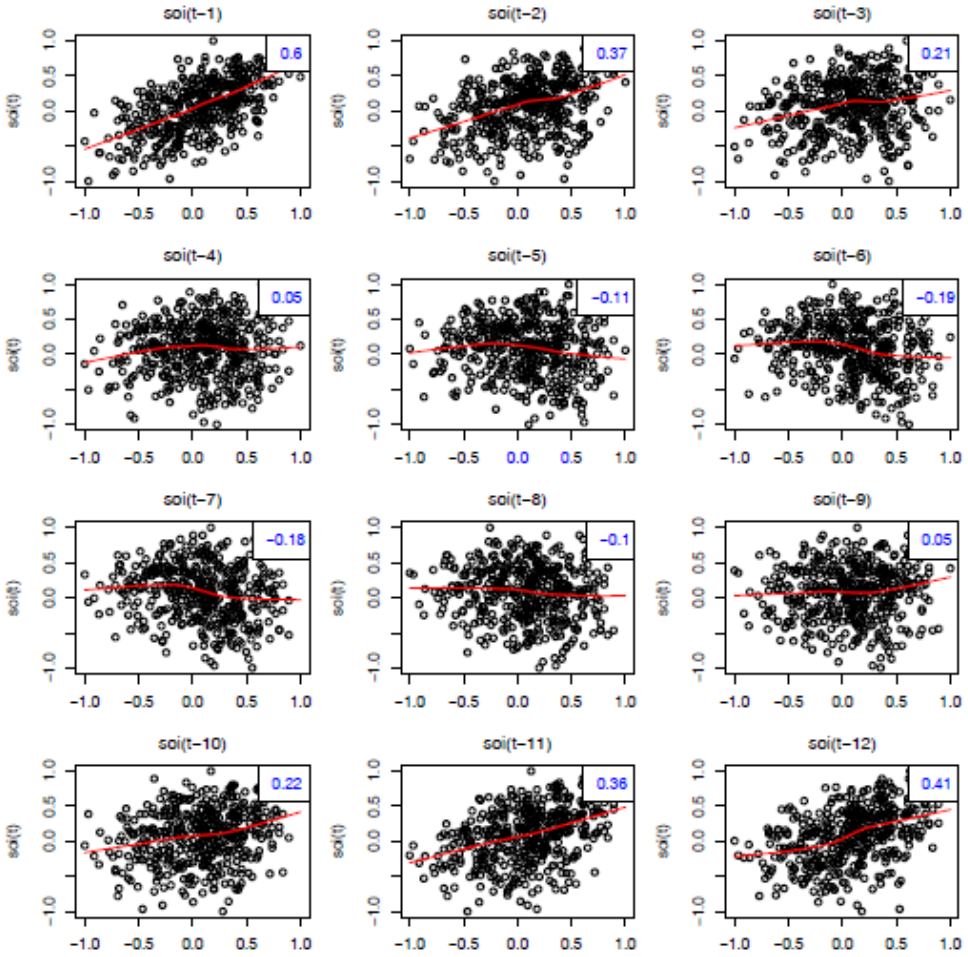

Fig. 2.7. Scatterplot matrix relating current SOI values, S_t, to past SOI values, S_{t-h}, at lags $h = 1, 2, ..., 12$. The values in the upper right corner are the sample autocorrelations and the lines are a lowess fit.

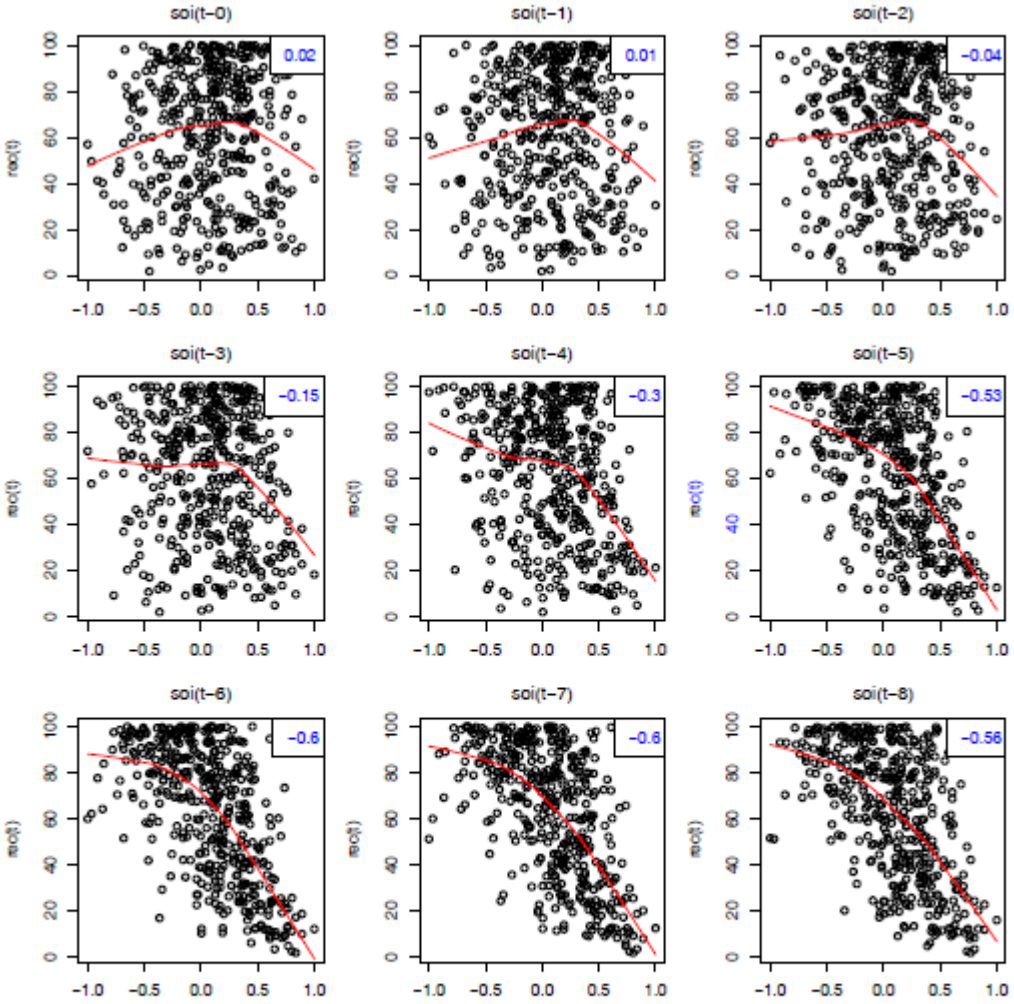

Fig. 2.8. Scatterplot matrix of the Recruitment series, R_t, on the vertical axis plotted against the SOI series, S_{t-h}, on the horizontal axis at lags $h = 0, 1, \ldots, 8$. The values in the upper right corner are the sample cross-correlations and the lines are a lowess fit.

Figure 2.8 shows a fairly strong nonlinear relationship between Recruitment, R_t, and the SOI series at $S_{t-5}, S_{t-6}, S_{t-7}, S_{t-8}$, indicating the SOI series tends to lead the Recruitment series and the coefficients are negative, implying that increases in the SOI lead to decreases in the Recruitment. The

nonlinearity observed in the scatterplots (with the help of the superimposed lowess fits) indicate that the behavior between Recruitment and the SOI is different for positive values of SOI than for negative values of SOI.

Example 2.8 Using Regression to Discover a Signal in Noise

In Example 1.12, we generated $n = 500$ observations from the model

$$x_t = A\cos(2\pi\omega t + \phi) + w_t, \tag{2.38}$$

where $\omega = 1/50$, $A = 2$, $\phi = .6\pi$, and $\sigma_w = 5$; the data are shown on the bottom panel of Figure 1.11 on page 16. At this point we assume the frequency of oscillation $\omega = 1/50$ is known, but A and ϕ are unknown parameters. In this case the parameters appear in (2.38) in a nonlinear way, so we use a trigonometric identity[4] and write

$$A\cos(2\pi\omega t + \phi) = \beta_1\cos(2\pi\omega t) + \beta_2\sin(2\pi\omega t),$$

where $\beta_1 = A\cos(\phi)$ and $\beta_2 = -A\sin(\phi)$. Now the model (2.38) can be written in the usual linear regression form given by (no intercept term is needed here)

$$x_t = \beta_1\cos(2\pi t/50) + \beta_2\sin(2\pi t/50) + w_t. \tag{2.39}$$

Using linear regression on the generated data, the fitted model is

$$\widehat{x}_t = -.71_{(.30)}\cos(2\pi t/50) - 2.55_{(.30)}\sin(2\pi t/50) \tag{2.40}$$

with $\widehat{\sigma}_w = 4.68$, where the values in parentheses are the standard errors. We note the actual values of the coefficients for this example are $\beta_1 = 2\cos(.6\pi) = -.62$ and $\beta_2 = -2\sin(.6\pi) = -1.90$. Because the parameter estimates are significant and close to the actual values, it is clear that we are able to detect the signal in the noise using regression, even though the signal appears to be obscured by the noise in the bottom panel of Figure 1.11. Figure 2.9 shows data generated by (2.38) with the fitted line, (2.40), superimposed.

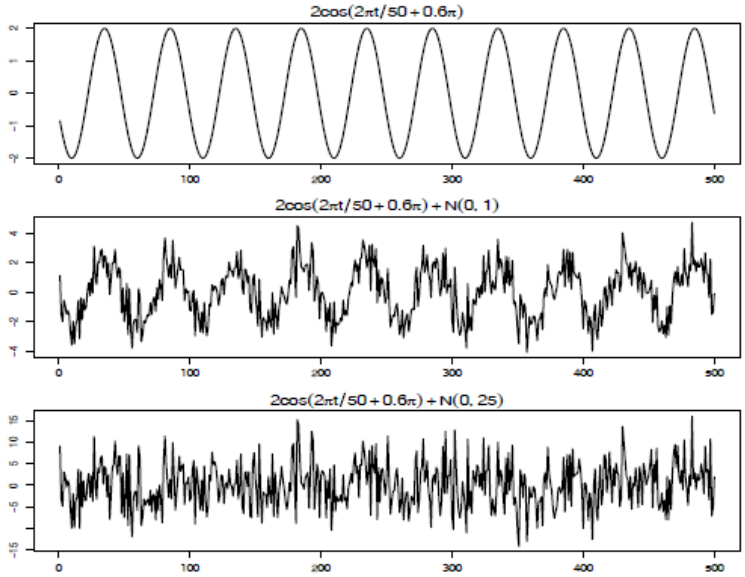

Fig. 1.11. Cosine wave with period 50 points (top panel) compared with the cosine wave contaminated with additive white Gaussian noise, $\sigma_w = 1$ (middle panel) and $\sigma_w = 5$ (bottom panel); see (1.5).

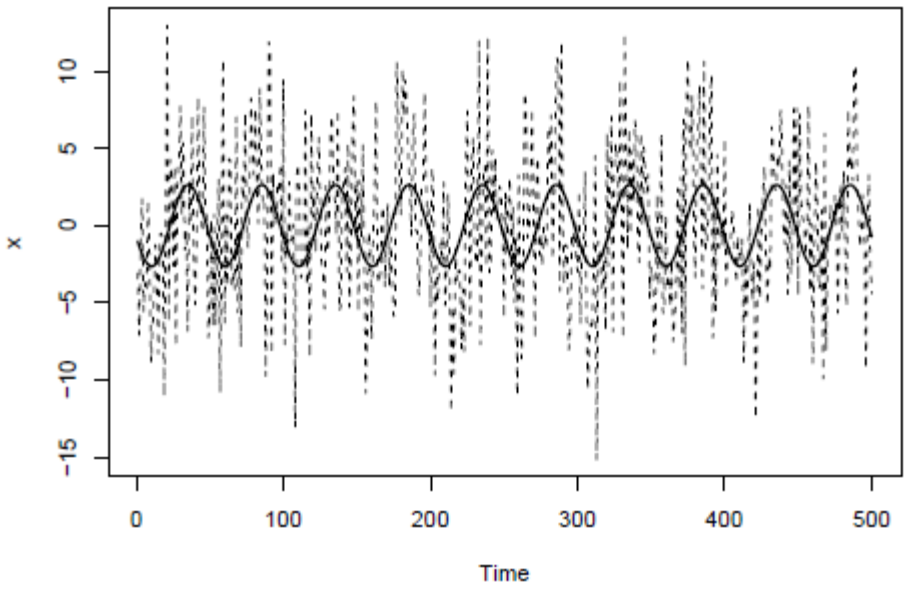

Fig. 2.9. Data generated by (2.38) [dashed line] with the fitted [solid] line, (2.40), superimposed.

Example 2.9 Using the Periodogram to Discover a Signal in Noise

The analysis in Example 2.8 may seem like cheating because we assumed we knew the value of the frequency parameter ω. If we do not know ω, we could try to fit the model (2.38) using nonlinear regression with ω as a parameter. Another method is to try various values of ω in a systematic way. Using the regression results of §2.2, we can show the estimated regression coefficients in Example 2.8 take on the special form given by

$$\widehat{\beta}_1 = \frac{\sum_{t=1}^{n} x_t \cos(2\pi t/50)}{\sum_{t=1}^{n} \cos^2(2\pi t/50)} = \frac{2}{n}\sum_{t=1}^{n} x_t \cos(2\pi t/50); \qquad (2.41)$$

$$\widehat{\beta}_2 = \frac{\sum_{t=1}^{n} x_t \sin(2\pi t/50)}{\sum_{t=1}^{n} \sin^2(2\pi t/50)} = \frac{2}{n}\sum_{t=1}^{n} x_t \sin(2\pi t/50). \qquad (2.42)$$

[5] In the notation of §2.2, the estimates are of the form $\sum_{t=1}^{n} x_t z_t \,/\, \sum_{t=1}^{n} z_t^2$ where $z_t = \cos(2\pi tj/n)$ or $z_t = \sin(2\pi tj/n)$. In this setup, unless $j = 0$ or $j = n/2$ if n is even, $\sum_{t=1}^{n} z_t^2 = n/2$; see Problem 2.10.

This suggests looking at all possible regression parameter estimates,[5] say

$$\widehat{\beta}_1(j/n) = \frac{2}{n}\sum_{t=1}^{n} x_t \cos(2\pi t\, j/n); \tag{2.43}$$

$$\widehat{\beta}_2(j/n) = \frac{2}{n}\sum_{t=1}^{n} x_t \sin(2\pi t\, j/n), \tag{2.44}$$

where, $n = 500$ and $j = 1, \ldots, \frac{n}{2} - 1$, and inspecting the results for large values. For the endpoints, $j = 0$ and $j = n/2$, we have $\widehat{\beta}_1(0) = n^{-1}\sum_{t=1}^{n} x_t$ and $\widehat{\beta}_1(\frac{1}{2}) = n^{-1}\sum_{t=1}^{n}(-1)^t x_t$, and $\widehat{\beta}_2(0) = \widehat{\beta}_2(\frac{1}{2}) = 0$.

For this particular example, the values calculated in (2.41) and (2.42) are $\widehat{\beta}_1(10/500)$ and $\widehat{\beta}_2(10/500)$. By doing this, we have regressed a series, x_t, of length n using n regression parameters, so that we will have a perfect fit. The point, however, is that if the data contain any cyclic behavior we are likely to catch it by performing these saturated regressions.

Next, note that the regression coefficients $\beta_1(j/n)$ and $\beta_2(j/n)$, for each j, are essentially measuring the correlation of the data with a sinusoid oscillating at j cycles in n time points.[6] Hence, an appropriate measure of the presence of a frequency of oscillation of j cycles in n time points in the data would be

$$P(j/n) = \widehat{\beta}_1^2(j/n) + \widehat{\beta}_2^2(j/n), \tag{2.45}$$

which is basically a measure of squared correlation. The quantity (2.45) is sometimes called the periodogram, but we will call $P(j/n)$ the scaled periodogram and we will investigate its properties in Chapter 4. Figure 2.10 shows the scaled periodogram for the data generated by (2.38), and it easily discovers the periodic component with frequency $\omega = .02 = 10/500$ even though it is difficult to visually notice that component in Figure 1.11 due to the noise.

Finally, we mention that it is not necessary to run a large regression

$$x_t = \sum_{j=0}^{n/2} \beta_1(j/n)\cos(2\pi t j/n) + \beta_2(j/n)\sin(2\pi t j/n) \tag{2.46}$$

to obtain the values of $\beta_1(j/n)$ and $\beta_2(j/n)$ [with $\beta_2(0) = \beta_2(1/2) = 0$] because they can be computed quickly if n (assumed even here) is a highly composite integer. There is no error in (2.46) because there are n observations and n parameters; the regression fit will be perfect.

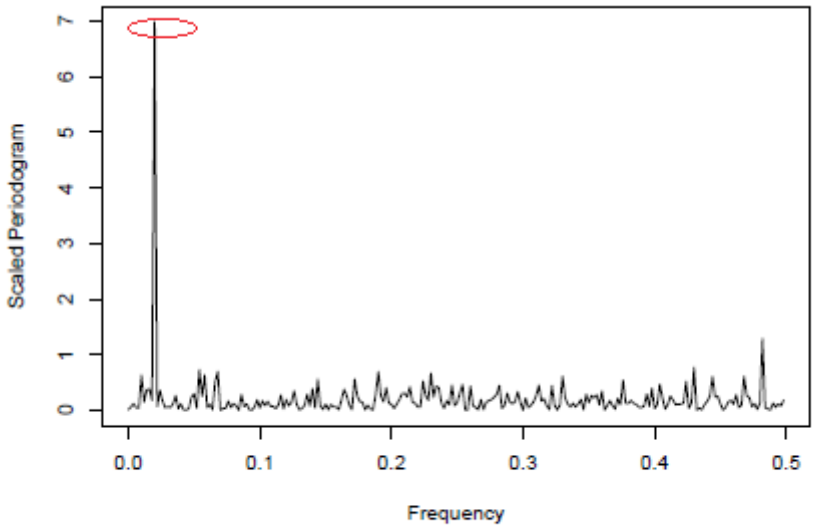

Fig. 2.10. The scaled periodogram, (2.45), of the 500 observations generated by (2.38); the data are displayed in Figures 1.11 and 2.9.

Smoothing in the Time Series Context

Using a moving average to smooth white noise. This method is useful in discovering certain traits in a time series, such as long-term trend and seasonal components. In particular, if x_t represents the observations, then

$$m_t = \sum_{j=-k}^{k} a_j x_{t-j}, \tag{2.50}$$

where $a_j = a_{-j} \geq 0$ and $\sum_{j=-k}^{k} a_j = 1$ is a symmetric moving average of the data.

Example 2.10 Moving Average Smoother

For example, Figure 2.11 shows the weekly mortality series discussed in Example 2.2, a five-point moving average (which is essentially a monthly average with $k = 2$) that helps bring out the seasonal component and a 53-point moving average (which is essentially a yearly average with $k = 26$) that helps bring out the (negative) trend in cardiovascular mortality. In both cases, the weights, $a_{-k}, \ldots, a_0, \ldots, a_k$, we used were all the same, and equal to $1/(2k + 1)$.[9]

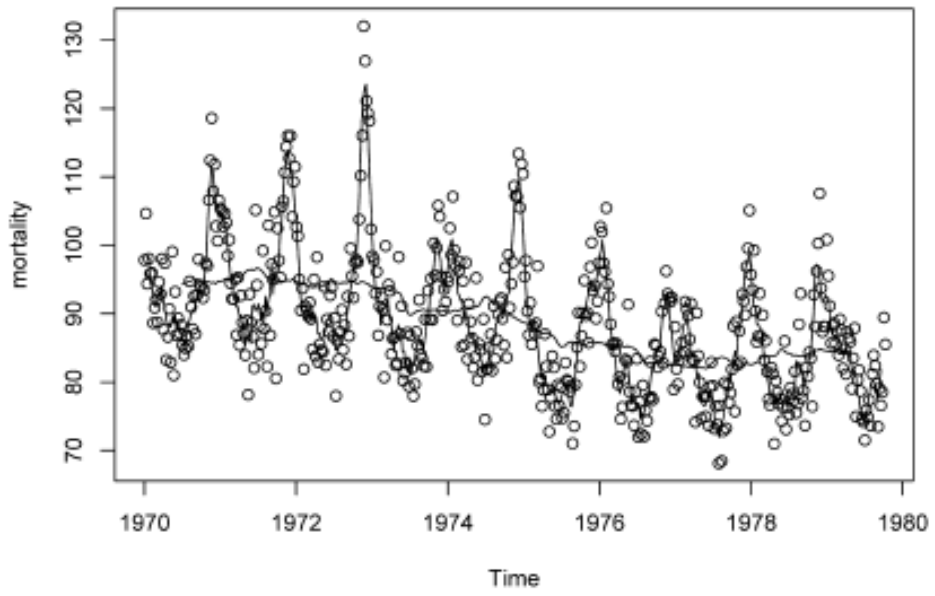

Fig. 2.11. The weekly cardiovascular mortality series discussed in Example 2.2 smoothed using a five-week moving average and a 53-week moving average.

Many other techniques are available for smoothing time series data based on methods from scatterplot smoothers. The general setup for a time plot is

$$x_t = f_t + y_t, \tag{2.51}$$

where f_t is some smooth function of time, and y_t is a stationary process. We may think of the moving average smoother m_t, given in (2.50), as an estimator of f_t. An obvious choice for f_t in (2.51) is polynomial regression

$$\boxed{f_t = \beta_0 + \beta_1 t + \cdots + \beta_p t^p.} \tag{2.52}$$

We have seen the results of a linear fit on the global temperature data in Example 2.1. For periodic data, one might employ periodic regression

$$\boxed{\begin{aligned} f_t = {} & \alpha_0 + \alpha_1 \cos(2\pi\omega_1 t) + \beta_1 \sin(2\pi\omega_1 t) \\ & + \cdots + \alpha_p \cos(2\pi\omega_p t) + \beta_p \sin(2\pi\omega_p t), \end{aligned}} \tag{2.53}$$

where $\omega_1, \ldots, \omega_p$ are distinct, specified frequencies. In addition, one might consider combining (2.52) and (2.53). These smoothers can be applied using classical linear regression.

Example 2.11 Polynomial and Periodic Regression Smoothers

Figure 2.12 shows the weekly mortality series with an estimated (via ordinary least squares) cubic smoother

$$\widehat{f}_t = \widehat{\beta}_0 + \widehat{\beta}_1 t + \widehat{\beta}_2 t^2 + \widehat{\beta}_3 t^3$$

superimposed to emphasize the trend, and an estimated (via ordinary least squares) cubic smoother plus a periodic regression

$$\widehat{f}_t = \widehat{\beta}_0 + \widehat{\beta}_1 t + \widehat{\beta}_2 t^2 + \widehat{\beta}_3 t^3 + \widehat{\alpha}_1 \cos(2\pi t/52) + \widehat{\alpha}_2 \sin(2\pi t/52)$$

superimposed to emphasize trend and seasonality.

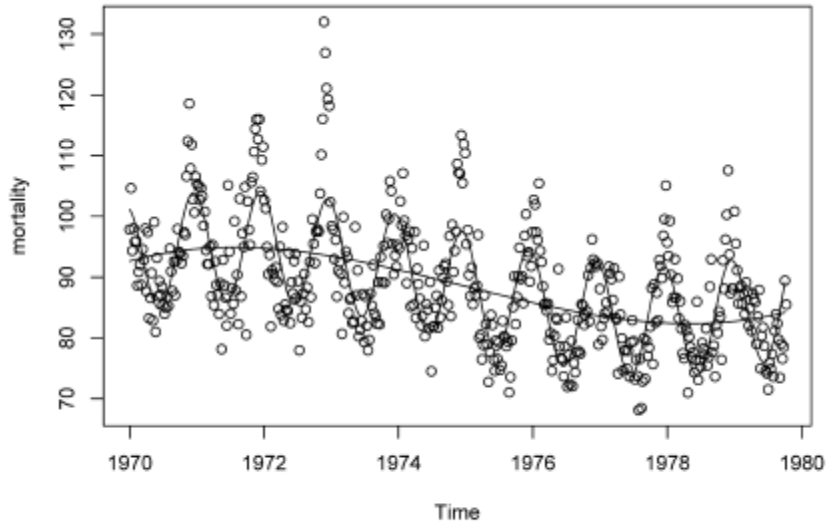

Fig. 2.12. The weekly cardiovascular mortality series with a cubic trend and cubic trend plus periodic regression.

Example 2.12 Kernel Smoothing

Kernel smoothing is a moving average smoother that uses a weight function, or kernel, to average the observations. Figure 2.13 shows kernel smoothing of the mortality series, where f_t in (2.51) is estimated by

$$\widehat{f}_t = \sum_{i=1}^{n} w_i(t) x_i, \tag{2.54}$$

where

$$w_i(t) = K\left(\tfrac{t-i}{b}\right) \Big/ \sum_{j=1}^{n} K\left(\tfrac{t-j}{b}\right). \tag{2.55}$$

are the weights and $K(\cdot)$ is a kernel function. This estimator, which was originally explored by Parzen (1962) and Rosenblatt (1956b), is often called the Nadaraya–Watson estimator (Watson, 1966); typically, the normal kernel, $K(z) = \frac{1}{\sqrt{2\pi}} \exp(-z^2/2)$, is used. To implement this in R, use the `ksmooth` function. The wider the bandwidth, b, the smoother the result. In Figure 2.13, the values of b for this example were $b = 5/52$ (roughly weighted two to three week averages because $b/2$ is the inner quartile range of the kernel) for the seasonal component, and $b = 104/52 = 2$ (roughly weighted yearly averages) for the trend component.

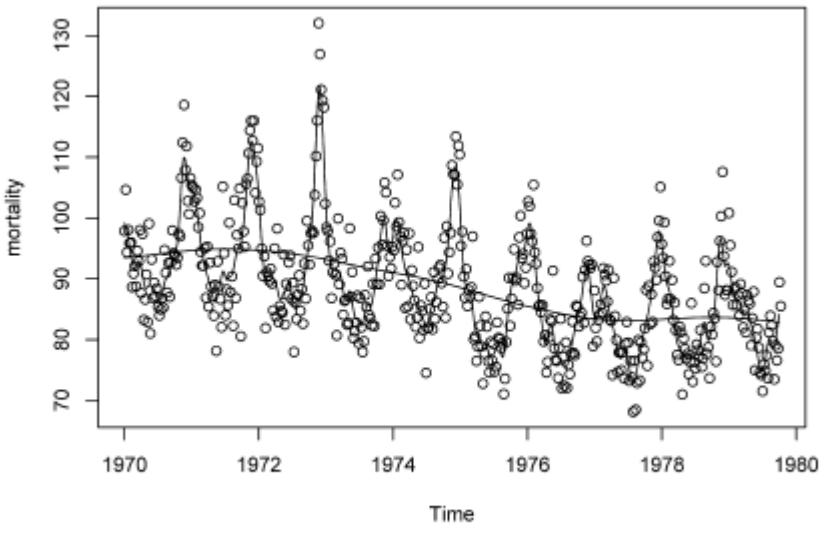

Fig. 2.13. Kernel smoothers of the mortality data.

Example 2.13 Lowess and Nearest Neighbor Regression

Another approach to smoothing a time plot is nearest neighbor regression. The technique is based on k-nearest neighbors linear regression, wherein one uses the data $\{x_{t-k/2}, \ldots, x_t, \ldots, x_{t+k/2}\}$ to predict x_t using linear regression; the result is $\widehat{f}_t$. For example, Figure 2.14 shows cardiovascular mortality and the nearest neighbor method using the R (or S-PLUS) smoother `supsmu`. We used $k = n/2$ to estimate the trend and $k = n/100$ to estimate the seasonal component. In general, `supsmu` uses a variable window for smoothing (see Friedman, 1984), but it can be used for correlated data by fixing the smoothing window, as was done here.

Lowess is a method of smoothing that is rather complex, but the basic idea is close to nearest neighbor regression. Figure 2.14 shows smoothing of mortality using the R or S-PLUS function `lowess` (see Cleveland, 1979). First, a certain proportion of nearest neighbors to x_t are included in a weighting scheme; values closer to x_t in time get more weight. Then, a robust weighted regression is used to predict x_t and obtain the smoothed estimate of f_t. The larger the fraction of nearest neighbors included, the smoother the estimate $\widehat{f}_t$ will be. In Figure 2.14, the smoother uses about two-thirds of the data to obtain an estimate of the trend component, and the seasonal component uses 2% of the data.

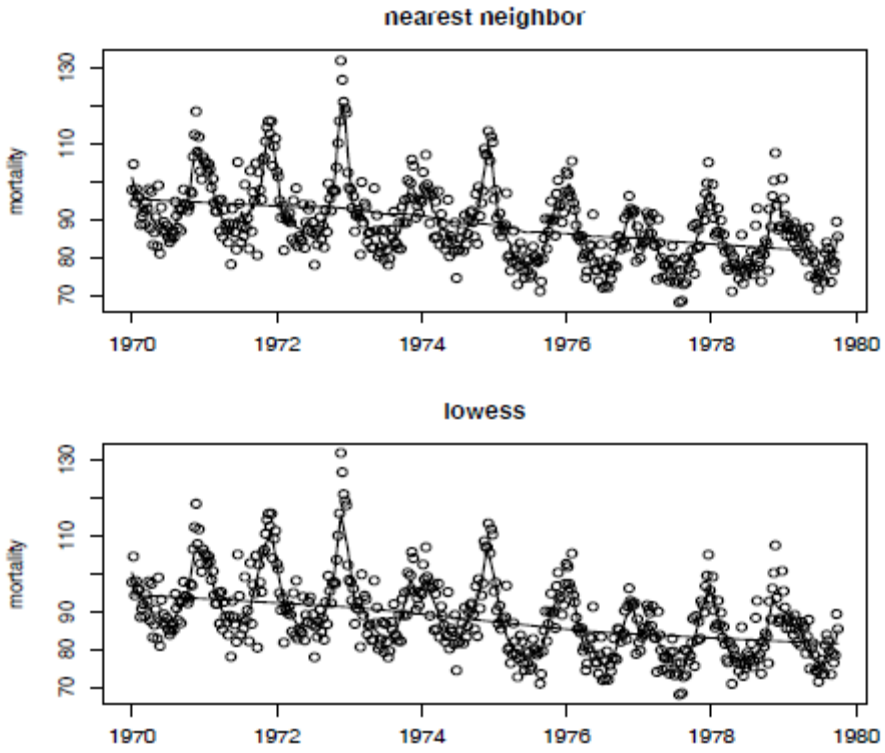

Fig. 2.14. Nearest neighbor (`supsmu`) and locally weighted regression (`lowess`) smoothers of the mortality data.

Suavização - Lowess

Lowess: Locally weighted regression scatter plot smoothing

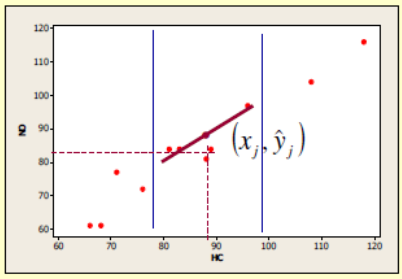

Para obter $(x_j, \hat{y}_j)$:

- Abrir uma faixa vertical centrada em (x_j,y_j), contendo *q=[fn]* pontos (0<f<1). Quando maior o valor de f, mais suave será o ajustamento. S-Plus

$$1/3 \le f \le 2/3$$

- Definir pesos para os pontos vizinhos de (x_j, y_j)

$$h(u) = \begin{cases} \left(1-|u|^3\right)^3 & \text{se } |u|<1 \\ 0 & \text{cc} \end{cases} \Rightarrow \text{o peso atribuído a } (x_k, y_k) \text{ é } h(x_k) = h\left(\frac{x_j - x_k}{d_j}\right)$$

distância *ao vizinho mais afastado*

- Ajustamos uma reta aos *q* pontos (M.Q.P.)

$$\hat{y}_j = \hat{\alpha} + \hat{\beta}\, x_j; \qquad \sum_{k=1}^{n} h(x_k)\,(y_k - \alpha - \beta x_k)^2$$

↑ resíduo:↓ peso

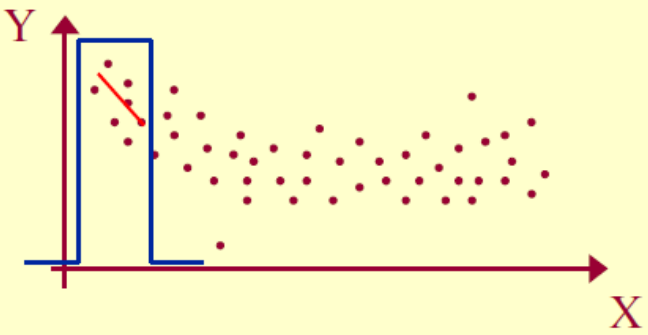

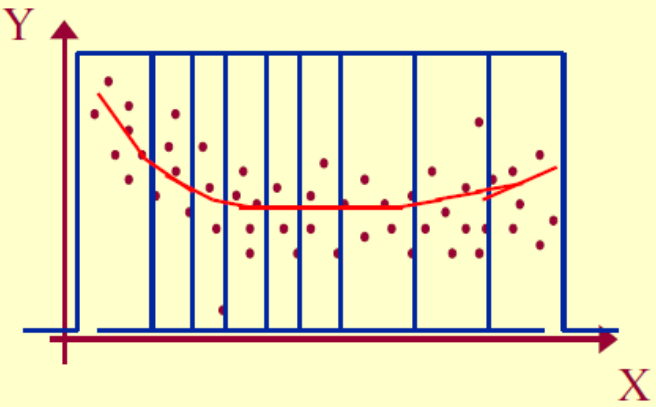

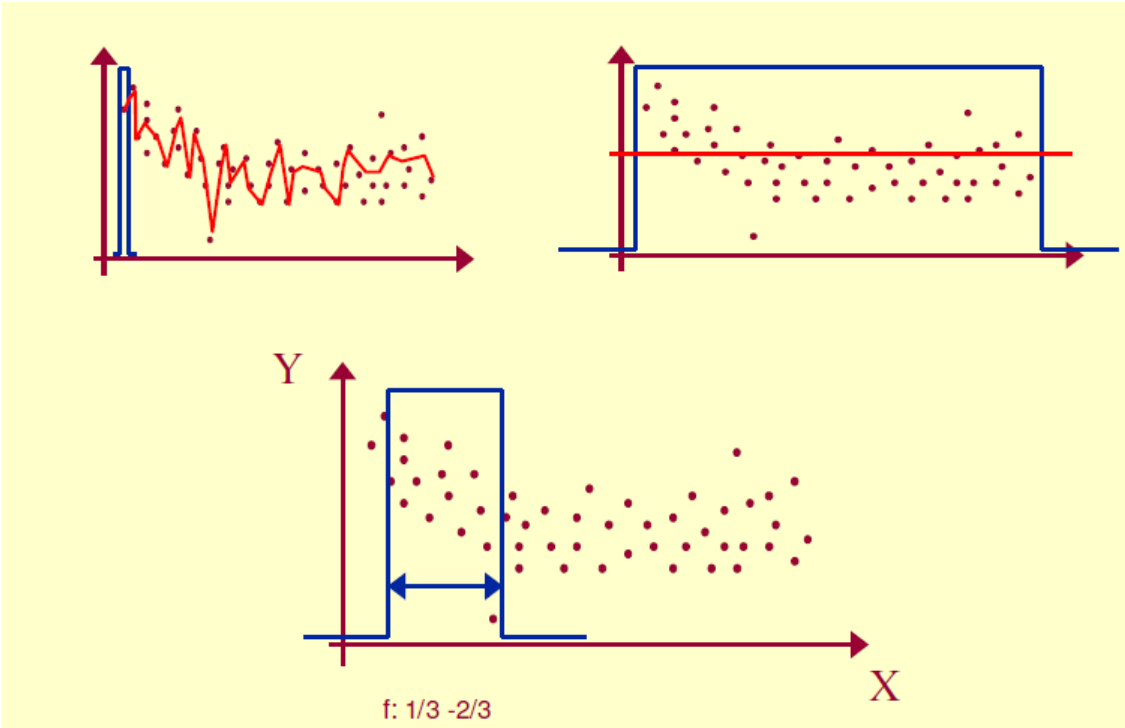

Suavização - Lowess

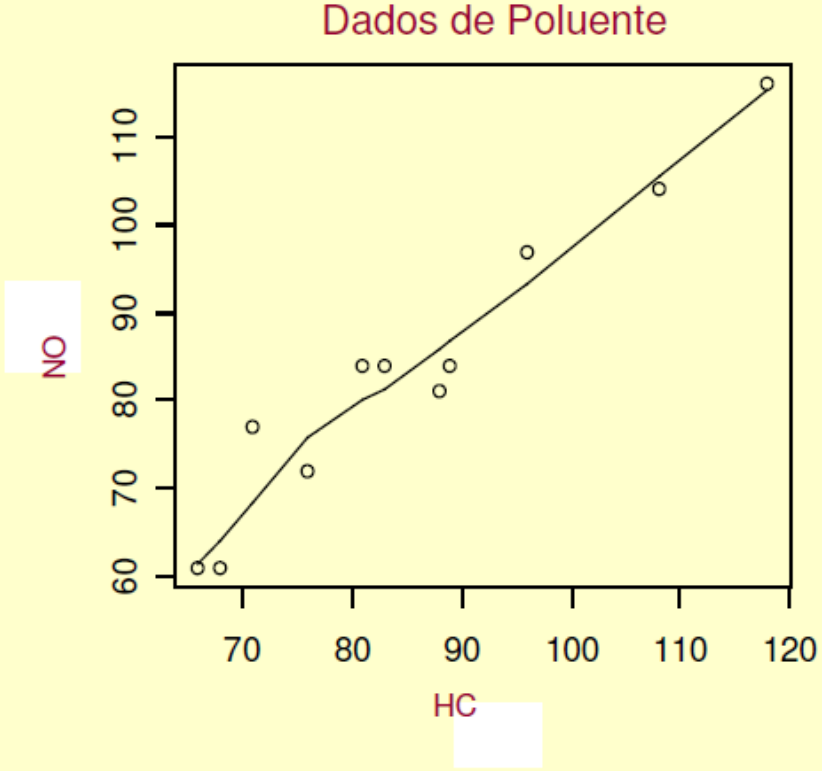


```
> plot (x,y)
> lines(lowess(x,y,f=2/3))
```

Suavização – Lowess Robusto

Na presença de valores atípicos ⇒ Lowess Robusto (Iterativo)

Atribuição de pesos robustos às observações (x_j, y_j)

h(u): Tri-cúbica

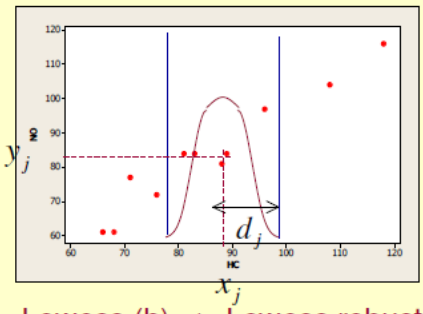

g(u): Bi-quadrática

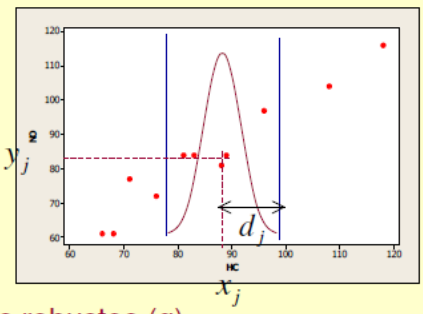

- Lowess (h) ⇒ Lowess robusto: pesos robustos (g)

$$\hat{\varepsilon}_j = y_j - \hat{y}_j \qquad Md: \text{mediana dos valores} |\hat{\varepsilon}_j|$$

$$g(u) = \begin{cases} (1-|u|^2)^2 & \text{se } |u|<1 \\ 0 & \text{cc} \end{cases} \Rightarrow \text{o peso atribuído a } (x_k, y_k) \text{ é } g(x_k) = g\left(\frac{\hat{\varepsilon}_k}{6Md}\right)$$

$$\hat{y}_j = \hat{\alpha} + \hat{\beta}\, x_j; \qquad \sum_{k=1}^{n} g\, h(x_k)\,(y_k - \alpha - \beta\, x_k)^2$$

Example 2.14 Smoothing Splines

An extension of polynomial regression is to first divide time $t = 1, \ldots, n$, into k intervals, $[t_0 = 1, t_1]$, $[t_1 + 1, t_2]$, $\ldots$, $[t_{k-1} + 1, t_k = n]$. The values $t_0, t_1, \ldots, t_k$ are called *knots*. Then, in each interval, one fits a regression of the form (2.52); typically, $p = 3$, and this is called cubic splines.

A related method is smoothing splines, which minimizes a compromise between the fit and the degree of smoothness given by

$$\sum_{t=1}^{n} [x_t - f_t]^2 + \lambda \int \left(f_t''\right)^2 dt, \tag{2.56}$$

where f_t is a cubic spline with a knot at each t. The degree of smoothness is controlled by $\lambda > 0$. There is a relationship between smoothing splines and state space models, which is investigated in Problem 6.7.

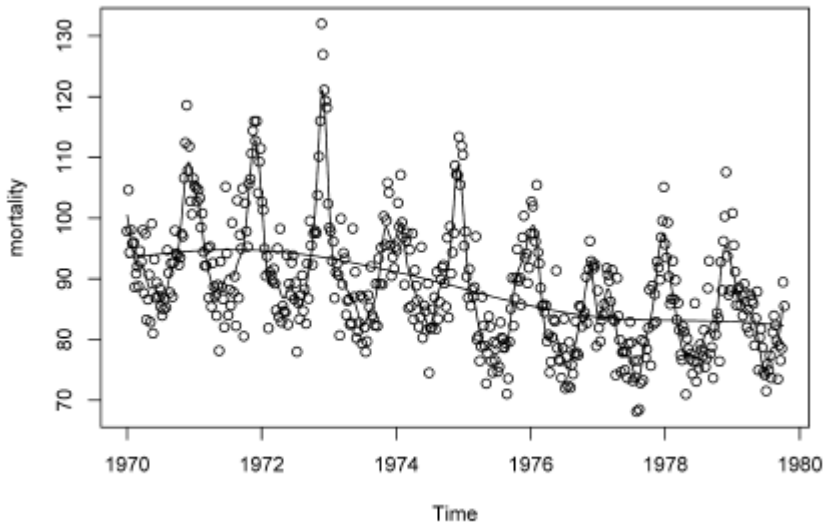

Fig. 2.15. Smoothing splines fit to the mortality data.

Example 2.15 Smoothing One Series as a Function of Another

In addition to smoothing time plots, smoothing techniques can be applied to smoothing a time series as a function of another time series. In this example, we smooth the scatterplot of two contemporaneously measured time series, mortality as a function of temperature. In Example 2.2, we discovered a nonlinear relationship between mortality and temperature. Continuing along these lines, Figure 2.16 shows scatterplots of mortality, M_t, and temperature, T_t, along with M_t smoothed as a function of T_t using lowess and using smoothing splines. In both cases, mortality increases at extreme temperatures, but in an asymmetric way; mortality is higher at colder temperatures than at hotter temperatures. The minimum mortality rate seems to occur at approximately 80° F.

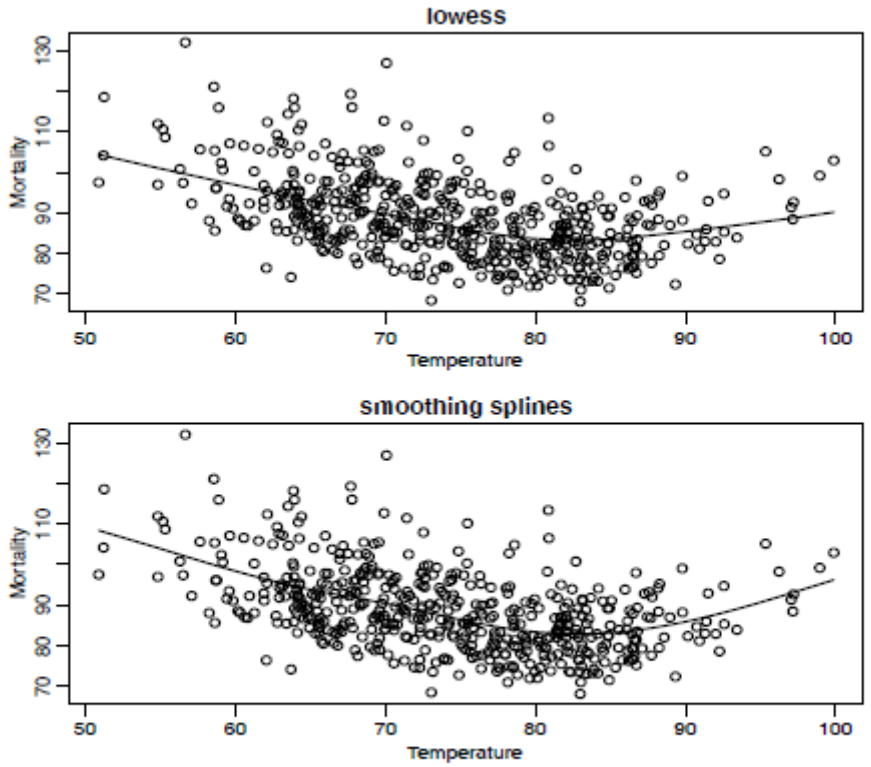

Fig. 2.16. Smoothers of mortality as a function of temperature using lowess and smoothing splines.

As a final word of caution, the methods mentioned in this section may not take into account the fact that the data are serially correlated, and most of the techniques have been designed for independent observations. That is, for example, the smoothers shown in Figure 2.16 are calculated under the false assumption that the pairs (Mt; Tt), are iid pairs of observations. In addition, the degree of smoothness used in the previous examples were chosen arbitrarily to bring out what might be considered obvious features in the data set.